Rotate to Scan: UNet-like Mamba with Triplet SSM Module for Medical Image Segmentation

Hao Tang, Lianglun Cheng, Guoheng Huang, Zhengguang Tan, Junhao Lu and Kaihong Wu

***Abstract*— Image segmentation holds a vital position in the realms of diagnosis and treatment within the medical domain. Traditional convolutional neural networks (CNNs) and Transformer models have made significant advancements in this realm, but they still encounter challenges because of limited receptive field or high computing complexity. Recently, State Space Models (SSMs), particularly Mamba and its variants, have demonstrated notable performance in the field of vision. However, their feature extraction methods may not be sufficiently effective and retain some redundant structures, leaving room for parameter reduction. Motivated by previous spatial and channel attention methods, we propose Triplet Mamba-UNet. The method leverages residual VSS Blocks to extract intensive contextual features, while Triplet SSM is employed to fuse features across spatial and channel dimensions. We conducted experiments on ISIC17, ISIC18, CVC-300, CVC-ClinicDB, Kvasir-SEG, CVC-ColonDB, and Kvasir-Instrument datasets, demonstrating the superior segmentation performance of our proposed TM-UNet. Additionally, compared to the previous VM-UNet, our model achieves a one-third reduction in parameters.**

***Index Terms*— U-Net, State Space Models, Medical image segmentation, Mamba**

I. Introduction

AUTOMATIC medical image segmentation plays a crucial role in disease diagnosis and surgery, which enables clinicians to accurately delineate anatomical structures, identify abnormalities, and plan surgical interventions with precision and efficiency [1]. Over the years, deep learning-based segmentation methods have performed remarkably, leveraging CNNs [2] and Transformer [3] as the cornerstone architecture. Among these, U-Net [4], renowned for its efficacy in segmenting medical images, has garnered widespread adoption and adaptation within the realm of medical imaging.

The U-shaped architecture stands as a pivotal framework lauded for its harmonious Encoder-Decoder design coupled with the integration of skip connections. It employs a hierarchical approach, utilizing multiple encoding layers to progressively extract features and transform high-dimensional images into low-dimensional representations. Meanwhile, symmetric decoding layers are used to decode these features gradually and map them back to high-dimensional space. Furthermore, the integration of skip connections facilitates the fusion of features from different hierarchical levels with their corresponding decoding layers, thereby enhancing the model's ability to capture fine-grained details and contextual information. Hence, a plethora of U-shaped architectures have begun to emerge. Initially, most researchers focused on modifications atop CNNs. However, due to the limited receptive fields of CNNs [5]–[7], which predominantly attend to local features, they failed to model long-range dependencies effectively, yielding marginal improvements. It was not until the advent of TransUNet [8] that the integration of transformer architecture within the U-shaped framework occurred, endowing encoders with the capability to capture long-distance information. The Medical Transformer [9] introduced a novel approach by utilizing consecutive transformer blocks as encoders and employing a patch-to-image training strategy, achieving results surpassing those obtained by pure convolutional methods. SwinUNet [10] represents the first U-shaped architecture solely based on transformers, surpassing the segmentation accuracy of both pure convolutional and hybrid transformer-convolution models. Furthermore, the U-shaped architecture has spawned several derivative models such as UNETR [11], DS-TransUNet [12], and UNet v2 [13].

Another issue has surfaced with the widespread integration of transformers: the substantial increase in computational complexity due to attention mechanisms, resulting in escalated model parameter counts and consequently prolonged inference and training times [14]. To address this issue, Gu et al. integrated the SSM [15] into an end-to-end neural network, resulting in Mamba [16], which exhibits rapid inference, with a throughput five times higher than that of transformers and demonstrates linear scaling in sequence length. VisionMamba [17] and VMamba [18] were the first to apply Mamba in computer vision. They respectively conducted selective scans on image patches in two and four directions, achieving performance comparable to Swin Transformer while significantly reducing time complexity. Subsequently, Mamba was integrated into U-shaped architectures [19]–[21], showcasing its competitiveness. Yet, these approaches lack methods akin to spatial attention mechanisms, thus failing to extract spatial fea-

This paragraph of the first footnote will contain the date on which you submitted your paper for review. It will also contain support information, including sponsor and financial support acknowledgment. For example, "This work was supported in part by the U.S. Department of Commerce under Grant BS123456."

Hao Tang, Lianglun Cheng, Guoheng Huang, Zhengguang Tan, Junhao Lu and Kaihong Wu are with the School of Computer Science and Technology, Guangdong University of Technology, Guangzhou 510006, China (e-mail: t1770134538@outlook.com; llcheng@gdut.edu.cn; kevinwong@gdut.edu.cn; bcbillycat@qq.com; polynya-code@outlook.com; zhexuejia123456@outlook.com).

tures effectively, let alone efficiently fuse channel features with spatial features. Additionally, despite the significantly reduced parameter count of these Mamba-based U-shaped architecture methods compared to transformer-based approaches, they still face some distance from practical application in downstream tasks, such as real-time segmentation during surgeries.

To address the challenge above, in this paper, we propose a lightweight module named Triplet SSM, incorporated into our modified model Triplet Mamba UNet (TM-UNet). Triplet SSM leverages the selective scan operation inherent in SSM to efficiently learn spatial relevant features. Diverging from conventional attention mechanisms, which often entail many additional learnable parameters, the Triplet SSM we propose explores strategies for constructing cost-effective yet impactful attention-like mechanisms while ensuring comparable or superior performance. Our focus lies in emphasizing the significance of capturing cross-dimensional interactions when performing selective scan operation, thereby facilitating the generation of comprehensive feature representations. Specifically, the feature maps are subjected to selective scan operations individually after undergoing multiple transpositions. Subsequently, the spatially relevant feature maps obtained are further fused with the channel-wise feature maps. In order to cut down parameter count, we enhance the bottleneck part of VM-UNet using Triplet SSM and modify its encoder and decoder structure, reducing parameters to two-thirds of the original while improving segmentation performance. Furthermore, we present the ResVSS block, an extension of the VSS block derived from VMamba, wherein residual connections are added at both ends. This augmentation facilitates the integration of a mechanism aimed at sharing global and local feature states to enhance performance, particularly on detailed images.

In summary, this paper makes the following contributions:

- We propose the lightweight feature fusion module, Triplet SSM, which, to the best of our knowledge, is the first attempt to use pure SSM to integrate spatial and channel features.
- We introduce the ResVSS block, which enhances the capability of VSS block to capture local and global features more comprehensively through residual connections.
- We perform VSS block, ResVSS block and Triplet SSM to propose TM-UNet, resulting in a reduction in parameters and an increase in mIOU from 79.82% to 80.51% on the ISIC17 dataset and from 80.45% to 81.55% on the ISIC18 dataset.

II. Related Work for Spatial-wise and Channel-wise Feature Fusion

The fusion of spatial-wise and channel-wise features has been a focal point in the advancement of medical image segmentation models, aiming to enhance the understanding of complex anatomical structures and abnormalities. Convolutional Block Attention Module (CBAM) [22] is the pioneering framework that integrates spatial and channel features. It comprises two primary components: the Channel Attention Module (CAM) and the Spatial Attention Module (SAM). The CAM recalibrates feature maps by capturing inter-channel dependencies, emphasizing channel-wise importance. Conversely, the SAM attends to informative spatial regions within feature maps, thereby focusing on intra-channel dependencies. DANet [23], unlike traditional methods that consider only local or global relationships, captures the interdependencies between any two positions in a feature map, allowing features from similar positions to contribute to each other's enhancement regardless of their distance. Coordinate attention [24] improves spatial awareness in neural networks by focusing on horizontal and vertical relationships within feature maps. By capturing feature distributions along each axis and compressing the information, it enhances spatial understanding without overwhelming the model with unnecessary technical complexity. The Bottleneck Attention Module (BAM) [25], similar to CBAM, seamlessly incorporates Channel and Spatial Attention Mechanisms to adaptively adjust channel feature responses, thereby accentuating both global and local information. After assimilating the characteristics of previous methods, Misra et al. introduced Triplet Attention [26], which employs a three-branch structure to capture cross-dimensional interactions for computing attention weights. For input tensors, Triplet Attention applies rotational operations followed by residual transformations to establish inter-dependencies among dimensions, encoding information across channels and spatial dimensions with negligible computational overhead. Moreover, in contrast to prior methods, Triplet Attention underscores the importance of multidimensional interactions without dimensionality reduction, thereby eliminating indirect correspondences between channels and weights. This renders Triplet Attention an efficient approach and inspires the present work.

III. Methodology

A. Preliminary

In contemporary SSM-based models, such as Structured State Space Sequence Models (S4) and Mamba, reliance is placed on a conventional continuous system. This system maps a one-dimensional input function or sequence, denoted as $x(t) \in \mathbb{R}$, through intermediary implicit states $h(t) \in \mathbb{R}^N$ to an output $y(t) \in \mathbb{R}$. This mapping process can be illustrated as a linear Ordinary Differential Equation (ODE):

$$\begin{aligned} h'(t) &= Ah(t) + Bx(t) \\ y(t) &= Ch(t) \end{aligned} \tag{1}$$

In this equation, $\mathbf{A} \in \mathbb{R}^{N\times N}$ represents the state matrix, while $\mathbf{B} \in \mathbb{R}^{N\times 1}$ and $\mathbf{C} \in \mathbb{R}^{N\times 1}$ denote the projection parameters.

S4 and Mamba discretize this continuous system to suit deep learning contexts better. They introduce a timescale parameter $\mathbf{\Delta}$ and convert $\mathbf{A}$ and $\mathbf{B}$ into discrete parameters $\overline{\mathbf{A}}$ and $\overline{\mathbf{B}}$ using a consistent discretization rule. The zero-order hold (ZOH) method is typically employed for discretization, outlined as follows:

$$\begin{aligned} \overline{\mathbf{A}} &= \exp(\mathbf{\Delta A}) \\ \overline{\mathbf{B}} &= (\mathbf{\Delta A})^{-1}(\exp(\mathbf{\Delta A}) - \mathbf{I}) \cdot \mathbf{\Delta B} \end{aligned} \tag{2}$$

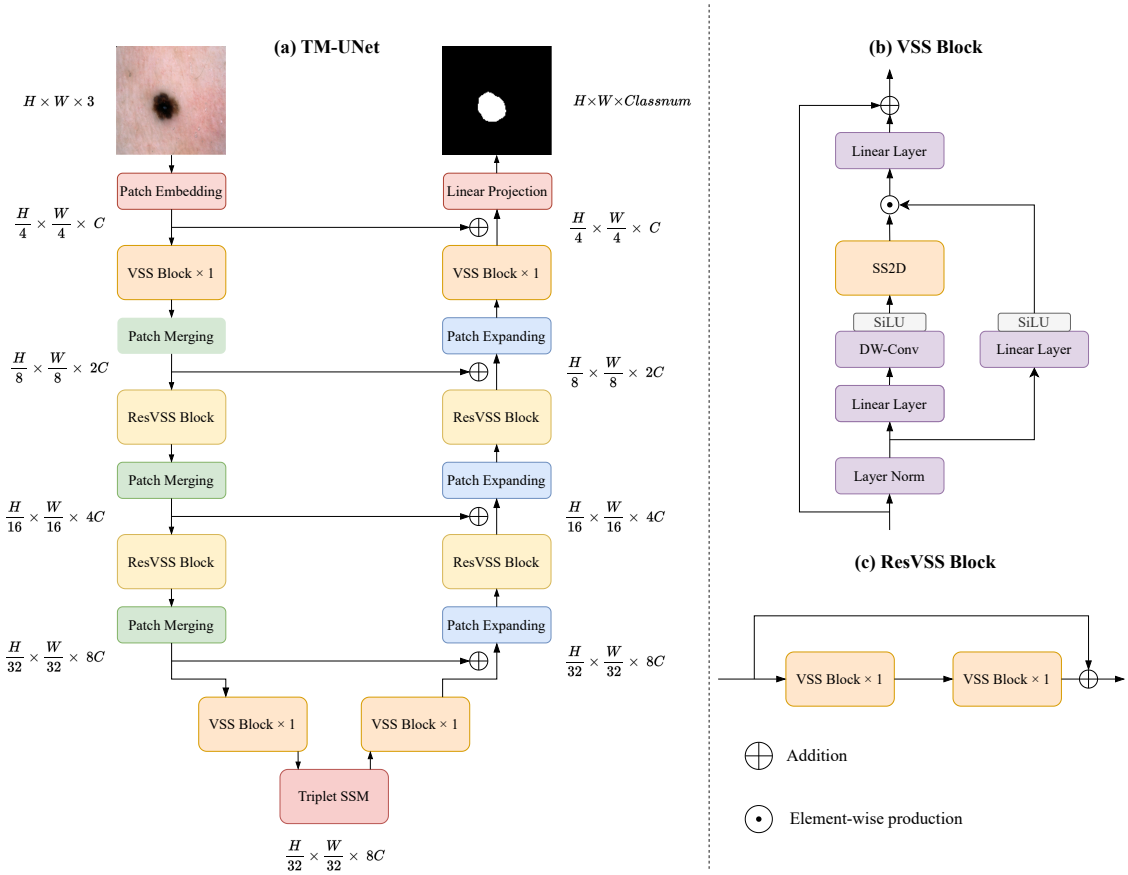

Fig. 1. (a) The overall architecture of our proposed TM-UNet. (b) The VSS block serves as the backbone of VM-UNet, with the SS2D operation constituting its core functionality. (c) ResVSS block comprises two consecutive VSS blocks, with a skip connection from the beginning to the end.

After discretization, SSM-based models can be computed using two distinct methods: linear recurrence or global convolution, denoted as equations (3).

$$\begin{aligned} h'(t) &= \overline{\mathbf{A}}h(t) + \overline{\mathbf{B}}x(t) \\ y(t) &= \mathbf{C}h(t) \\ \overline{K} &= \left(\mathbf{C}\overline{\mathbf{B}}, \mathbf{C}\overline{\mathbf{A}\mathbf{B}}, \ldots, \mathbf{C}\overline{\mathbf{A}}^{L-1}\overline{\mathbf{B}}\right) \\ y &= x * \overline{\mathbf{K}} \end{aligned} \tag{3}$$

Here, $\overline{\mathbf{K}} \in \mathbb{R}^L$ represents a structured convolutional kernel, and L denotes the length of the input sequence x.

B. Overview of the TM-UNet

The overall architecture of TM-UNet, illustrated in Fig .1 (a), adopts a symmetrical design comprising patch embedding, encoder, bottleneck, decoder, and a final linear projection layer. Given an input image $x \in \mathbb{R}^{H\times W\times 3}$, the patch embedding layer amalgamates every non-overlapping 4x4 pixel region into an image patch and projects its channel dimension to C. Consequently, the processed feature map reshapes to $\frac{h}{4} \times \frac{w}{4} \times C$, where h and w denote the height and width of the input image, respectively. This transformation facilitates efficient representation of local image information while reducing computational complexity. Subsequently, the feature map undergoes feature extraction through four stages of VSS blocks. Here, the VSS blocks maintain the shape of the feature map but, via the patch merging module, reduce the height and width by half with each pass while doubling the number of channels. Consequently, the output shape of each stage within the encoder progresses sequentially as $\frac{H}{4} \times \frac{W}{4} \times C$, $\frac{H}{8} \times \frac{W}{8} \times 2C$, $\frac{H}{16} \times \frac{W}{16} \times 4C$, and $\frac{H}{32} \times \frac{W}{32} \times 8C$. The features are fed into the decoder following the Triplet SSM as the bottleneck layer. The shape transformation in the decoder is conversely executed, with the final linear projection layer projecting the shape $\frac{H}{4} \times \frac{W}{4} \times C$ to $H \times W \times Classnum$.

Before each VSS block in the encoder, a skip connection is established to connect with the corresponding location in the decoder. These skip connections facilitate the propagation of information from earlier encoder stages to later decoder stages, aiding in preserving and utilizing low-level features throughout the network.

C. VSS Block and ResVSS Block

The VSS block, originating from VMamba and serving as the backbone of the TM-UNet encoder and decoder, is depicted in Fig. 1(b). Initially, the input undergoes processing through an initial linear embedding layer, following which it branches into two separate information streams. One stream undergoes a 3 × 3 depth-wise convolution [27] layer and subsequently a Silu activation [28] function before entering the main 2D-Selective-Scan (SS2D) module. The output of the SS2D module then passes through a layer normalization and is

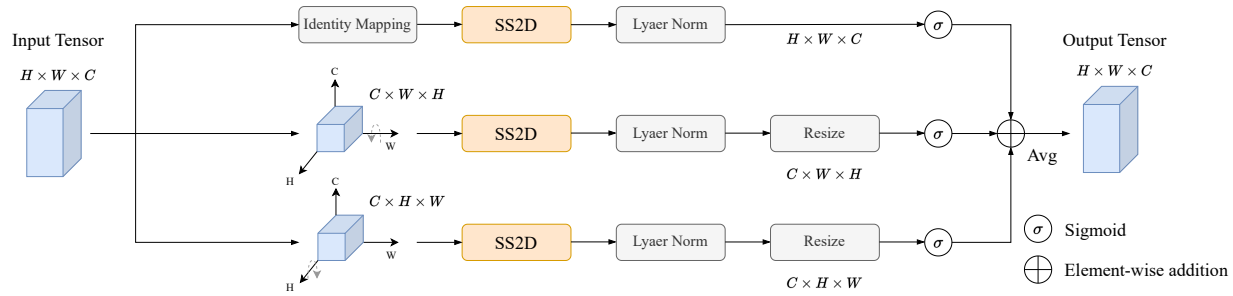

Fig. 2. Illustration of our proposed Triplet SSM, comprising three branches. The upper branch extracts the channel feature of the input tensor. The middle branch captures spatial information across channel dimension C and width dimension W. The lowest branch handles the height dimension H and the channel dimension C.

combined with the output from the other information stream, which has also undergone Silu activation. This merged output constitutes the final result of the VSS block. The process of the VSSBlock can be represented by the following formula:

$$\begin{aligned} \hat{x} &= \alpha_1(\gamma(x)) \\ \hat{y} &= \alpha_2(\sigma_1(\psi(W * \hat{x} + b)) \otimes \sigma_2(\hat{x})) + x \end{aligned} \tag{4}$$

Where γ denotes layer normalization, α represents the linear layer, W and b signify the kernel and bias in Depthwise Convolution respectively, σ indicates the SiLU activation function, $\otimes$ denotes element-wise multiplication, and ψ represents the SSM operations.

Building upon the foundation of the VSS block, we introduce the ResVSS block, shown in Fig .1(c), which comprises two consecutive VSS blocks connected via a residual connection, facilitating the transfer of shallow-level information via identity mapping to deeper layers. The process is defined as follows:

$$y = V_1(V_2(x)) + x \tag{5}$$

Here, x and y are the input and output tensors, V_1 and V_2 denote the first VSS block and the second.

D. Triplet SSM

As depicted in Fig. 2, our Triplet SSM structure is designed to process an input tensor $z \in R^{H\times W\times C}$. The input tensor is processed separately by three branches. In the first branch, no transformation is applied to the tensor; instead, it undergoes the SS2D module. This branch aims to capture channel features independent of spatial information. The tensor is rotated 90 degrees clockwise along the W-axis in the second branch, denoted as $z_1^* \in R^{C\times W\times H}$. Subsequently, SS2D operations are performed, extracting features from the channel and H dimensions and establishing spatial correlations. Similarly, in the third branch, the tensor is rotated 90 degrees counterclockwise along the H-axis, denoted as $z_2^* \in R^{C\times W\times H}$. SS2D operations are then applied to extract features from the channel and W dimensions. Layer normalization and sigmoid function follow each SSM operation. The tensors obtained from z_1 and z_2 are resized to their initial shapes for element-wise addition with the tensor obtained from z, followed by averaging to yield the final output tensor, maintaining the same shape as the input.

In general, all operations of the Triplet SSM can be represented by the following equations:

$$Z = \frac{1}{3}(\overline{\sigma_1(\gamma_1(\psi_1(z_1^*)))} + \overline{\sigma_2(\gamma_2(\psi_2(z_2^*)))} + \sigma_3(\gamma_3(\psi_3(z_3)))) \tag{6}$$

Where the ψ represents the SSM operations; γ represents layer normalization, and the σ represents the sigmoid activation function, utilized for learning the weights of each feature in the final output tensor. The equation can be further simplified to equation (7):

$$Z = \frac{1}{3}(\overline{Z_1} + \overline{Z_2} + Z_3) \tag{7}$$

Here, $\overline{Z1}$ and $\overline{Z2}$ represent the outputs from SS2D after the resize operation.

Besides the SS2D module, no linear, convolutional layers or multiplication operations are utilized in the Triplet SSM. Therefore, the computational cost associated with this module is relatively low. Furthermore, the introduction of spatial-related information enables the model to acquire more comprehensive knowledge, leading to improved performance in instance segmentation metrics, as detailed in the ablation experiments section.

E. Loss function

Since the image masks utilized in our medical image segmentation are binary, the segmentation task can be regarded as a pixel-wise binary classification. Hence, we employ a combination of Binary Cross Entropy and DICE loss as the overall loss function, as represented by equations (8).

$$\begin{aligned} L_{Bce} &= -\frac{1}{N}\sum_{1}^{N}\left[y_i \log\left(\hat{y}_i\right) + \left(1-y_i\right)\log\left(1-\hat{y}_i\right)\right] \\ L_{\text{Dice}} &= 1 - \frac{2|X \cap Y|}{|X| + |Y|} \\ L_{\text{BceDice}} &= \lambda_1 L_{\text{Bce}} + \lambda_2 L_{\text{Dice}} \end{aligned} \tag{8}$$

where N denotes the total number of samples. y_i represents the ground truth and $\hat{y}_i$ represents the predicted value. $|X|$ and $|Y|$ denote the predicted values and ground truth, respectively. ϕ_1 and ϕ_2 are both trial values typically set to 1.

TABLE I
QUATITATIVE COMPARISON BETWEEN TM-UNET AND OTHER METHODS FOR ISIC 2017 AND ISIC 2018(BOLD INDICATES THE BEST.)

Dataset	Model	mIoU(%)↑	DSC(%)↑	Acc(%)↑	Spe(%)↑	Sen(%)↑
ISIC17	UNet	76.98	86.99	95.65	97.43	86.82
	UTNetV2	77.35	87.23	95.84	98.05	84.85
	TransFuse	79.21	88.40	96.17	97.98	87.14
	MALUNet	78.78	88.13	96.18	**98.47**	84.78
	VM-UNet	79.82	88.52	96.34	97.96	87.65
	VM-UNetV2	79.73	88.14	96.09	97.78	**87.89**
	TM-UNet	**80.51**	**89.20**	**96.46**	98.28	87.37
ISIC18	UNet	77.86	87.55	94.05	96.69	85.86
	Unet++	78.31	87.83	94.02	95.75	88.65
	Att-Unet	78.43	87.91	94.13	96.23	87.6
	UTNetV2	78.97	88.25	94.32	96.48	87.6
	SANet	79.52	88.59	94.39	95.97	89.46
	TransFuse	80.63	89.27	94.66	95.74	**91.28**
	MALUNet	80.25	89.04	94.62	96.19	89.74
	UNetV2	80.71	89.32	94.86	**96.94**	88.34
	VM-Unet	80.21	88.69	94.57	96.15	90.32
	VM-UNetV2	80.45	88.73	94.76	96.51	88.57
	TM-UNet	**81.55**	**89.84**	**95.08**	96.68	89.98

TABLE II
COMPARATIVE EXPERIMENTAL RESULTS ON THE KVASIR-INSTRUMENT, KVASIR-SEG, CLINICDB, COLONDB, AND CVC-300 DATASETS(BOLD INDICATES THE BEST)

Dataset	Model	mIoU(%)↑	DSC(%)↑	Acc(%)↑	Spe(%)↑	Sen(%)↑
Kvasir-Instrument	VM-UNet	88.67	93.99	98.90	**99.55**	92.51
	VM-UNetV2	87.30	93.22	98.75	99.41	92.33
	TM-UNet	**89.57**	**94.50**	**98.97**	99.44	**94.48**
Kvasir-SEG	VM-UNet	**78.66**	**88.05**	**96.61**	**98.96**	83.27
	VM-UNetV2	76.99	87.00	96.12	97.81	**86.55**
	TM-UNet	77.83	87.53	96.37	98.37	85.02
ClinicDB	VM-UNet	76.53	86.71	97.92	99.05	84.89
	VM-UNetV2	83.80	91.19	98.59	99.22	**91.35**
	TM-UNet	**83.82**	**91.20**	**98.59**	**99.25**	91.10
ColonDB	VM-UNet	51.17	67.70	95.55	98.19	62.67
	VM-UNetV2	51.89	68.32	95.31	97.52	67.85
	TM-UNet	**57.23**	**72.80**	**96.26**	**98.58**	**98.37**
CVC-300	VM-UNet	68.57	81.35	98.68	99.12	85.89
	VM-UNetV2	72.30	83.92	98.81	99.03	92.51
	TM-UNet	**77.79**	**87.51**	**99.11**	**99.32**	**92.94**

IV. EXPERIMENTS

We conducted extensive experiments on the TM-UNet, employing datasets covering skin lesions, intestinal polyps, and surgical instrument segmentation.

A. Datasets

ISIC17 [28] and ISIC18 [29] datasets are two extensive collections of dermoscopic images developed by the International Skin Imaging Collaboration (ISIC), aimed at aiding researchers in devising image analysis tools for the automated diagnosis of melanoma from dermoscopic images. The ISIC17 dataset comprises 2150 images, while ISIC18 includes 2694 images, with a partitioning of these images into training and validation sets at a 7:3 ratio.

Concerning the polyp dataset, we employed five publicly available datasets. Our training set consists of 900 images from Kvasir-SEG and 550 images from CVC-ClinicDB, totaling 1450 samples. The test set comprises four subsets: the remaining 100 images from Kvasir-SEG, the remaining 62 images from CVC-ClinicDB, the complete CVC-ColonDB dataset (380 samples), and 60 from the CVC-300 dataset.

Additionally, we utilized the Kvasir instrument dataset, designed specifically for medical instrument segmentation in

TABLE III
PARAMS COMPARATIONS(BOLD INDICATES THE BEST)

Model	Params(M)↓	FLOPs(G)↓	Total Params(M)↓
VM-UNet	22.08	4.73	27.50
VM-UNetV2	17.91	4.40	22.77
TM-UNet	**14.86**	**3.42**	**18.41**

TABLE IV
ABLATION STUDIES ON TRIPLET SSM MODULE AND RESIDUAL CONNECTION(BOLD INDICATES THE BEST)

Datasets	configurations	Total Params(M)↓	mIoU(%)↑	DSC(%)↑	Acc(%)↑	Spe(%)↑	Sen(%)↑
ISIC17	(a)	18.41	76.88	86.93	95.74	97.96	84.68
	(b)	18.41	79.89	88.82	96.27	97.84	**88.49**
	(c)	18.41	**80.51**	**89.20**	**96.46**	**98.28**	87.37
ISIC18	(a)	18.41	78.82	88.15	94.15	95.66	89.43
	(b)	18.41	81.01	89.51	94.92	**96.79**	89.09
	(c)	18.41	**81.55**	**89.84**	**95.08**	96.68	**89.98**

gastrointestinal surgery.

B. Implemention Details

The model was trained on a system running Ubuntu 22.04.3, with Python 3.8, CUDA 11.8, and an RTX 4090 GPU (24GB). Before feeding the images into the model, we resized them to 256x256 and applied random flipping and rotation operations for data augmentation. We employed the AdamW [30] optimizer with an initial learning rate of 1e-3, along with the CosineAnnealingLR scheduler, with a maximum of 50 iterations and a minimum learning rate of 1e-5. The VMamba-S pre-trained weights were utilized as the initial weights for the TM-UNet encoder and decoder. We maintained a uniform batch size of 32 for all datasets used and trained for 300 epochs.

C. Comparison Results

We compared TM-UNet with several existing methods. As shown in Table I, our approach demonstrated superior performance over the previous state-of-the-art models, VM-UNet and VM-UNetV2, across various metrics including mIoU, DSC, and Acc on the ISIC17 and ISIC18 datasets. Additionally, according to Table II, our method exhibited noteworthy advancements over VM-UNet and VM-UNetV2 on the polyp and Kvasir instrument datasets, particularly in the ColonDB and CVC-300 datasets, which brought improvement up to 6.54% and 5.49% respectively.

Furthermore, we also compared the parameter counts of the models, as detailed in Table III. When the input size of the models was fixed at (3,256,256), our method exhibited the fewest learnable parameters and floating-point operations, reducing memory consumption greatly.

D. Ablation Study

To investigate the effectiveness of the ResVSS block and Triplet SSM, we conducted ablation experiments on the ISIC 2017 and ISIC 2018 datasets. The models in the experiment were configured as follows: (a) a modified VM-UNet serving as the baseline, with each stage of the encoder and decoder containing 1, 2, 2, and 1 VSS block, respectively; (b) integration of Triplet SSM into the baseline's bottleneck section; and (c) addition of residual connections before and after the encoder and decoder with a depth of 2, forming the proposed TM-UNet.

From Table IV, it is evident that the proposed ResVSS block and Triplet SSM in this study almost incur few increase in parameter count while significantly improving mIoU and DSC, which validates the proposed approach's effectiveness.

V. CONCLUSION

In this paper, we propose a pure SSM-based U-shaped architecture model, TM-UNet, utilizing residual VSS blocks as encoder and decoder, and Triplet SSM as the bottleneck. Extensive experimental results demonstrate that TM-UNet exhibits superior performance compared to previous SSM-based U-shaped models with fewer parameters. In the future, we plan to explore weakly supervised learning and further reduce model parameters, significantly reducing the requirements for training data and computational resources, with the aim of deploying TM-UNet in broader applications.

REFERENCES

[1] J.-Z. Cheng, D. Ni, Y.-H. Chou, J. Qin, C.-M. Tiu, Y.-C. Chang, C.-S. Huang, D. Shen, and C.-M. Chen, "Computer-aided diagnosis with deep learning architecture: Applications to breast lesions in us images and pulmonary nodules in ct scans," *Scientific Reports*, vol. 6, 2016.

[2] Y. LeCun and Y. Bengio, *Convolutional networks for images, speech, and time series*, p. 255–258. Cambridge, MA, USA: MIT Press, 1998.

[3] O. Ronneberger, P. Fischer, and T. Brox, "U-net: Convolutional networks for biomedical image segmentation," in *Medical Image Computing and Computer-Assisted Intervention – MICCAI 2015* (N. Navab, J. Hornegger, W. M. Wells, and A. F. Frangi, eds.), (Cham), pp. 234–241, Springer International Publishing, 2015.

[4] A. Vaswani, N. M. Shazeer, N. Parmar, J. Uszkoreit, L. Jones, A. N. Gomez, L. Kaiser, and I. Polosukhin, "Attention is all you need," in *Neural Information Processing Systems*, 2017.

[5] X. Xiao, S. Lian, Z. Luo, and S. Li, "Weighted res-unet for high-quality retina vessel segmentation," in *2018 9th International Conference on Information Technology in Medicine and Education (ITME)*, pp. 327–331, 2018.

[6] S. Guan, A. A. Khan, S. Sikdar, and P. V. Chitnis, "Fully dense unet for 2-d sparse photoacoustic tomography artifact removal," *IEEE Journal of Biomedical and Health Informatics*, vol. 24, pp. 568–576, 2018.

[7] N. Ibtehaz and M. S. Rahman, "MultiResUNet : Rethinking the U-Net architecture for multimodal biomedical image segmentation," *Neural Netw*, vol. 121, pp. 74–87, Jan 2020.

[8] J. Chen, Y. Lu, Q. Yu, X. Luo, E. Adeli, Y. Wang, L. Lu, A. L. Yuille, and Y. Zhou, "Transunet: Transformers make strong encoders for medical image segmentation," *ArXiv*, vol. abs/2102.04306, 2021.

[9] J. M. J. Valanarasu, P. Oza, I. Hacihaliloglu, and V. M. Patel, "Medical transformer: Gated axial-attention for medical image segmentation," in *Medical Image Computing and Computer Assisted Intervention – MICCAI 2021* (M. de Bruijne, P. C. Cattin, S. Cotin, N. Padoy, S. Speidel, Y. Zheng, and C. Essert, eds.), (Cham), pp. 36–46, Springer International Publishing, 2021.

[10] H. Cao, Y. Wang, J. Chen, D. Jiang, X. Zhang, Q. Tian, and M. Wang, "Swin-unet: Unet-like pure transformer for medical image segmentation," in *Computer Vision – ECCV 2022 Workshops* (L. Karlinsky, T. Michaeli, and K. Nishino, eds.), (Cham), pp. 205–218, Springer Nature Switzerland, 2023.

[11] A. Hatamizadeh, Y. Tang, V. Nath, D. Yang, A. Myronenko, B. Landman, H. R. Roth, and D. Xu, "Unetr: Transformers for 3d medical image segmentation," in *2022 IEEE/CVF Winter Conference on Applications of Computer Vision (WACV)*, (Los Alamitos, CA, USA), pp. 1748–1758, IEEE Computer Society, jan 2022.

[12] A. Lin, B. Chen, J. Xu, Z. Zhang, G. Lu, and D. Zhang, "Ds-transunet: Dual swin transformer u-net for medical image segmentation," *IEEE Transactions on Instrumentation and Measurement*, vol. 71, pp. 1–15, 2022.

[13] Y. Peng, M. Sonka, and D. Z. Chen, "U-net v2: Rethinking the skip connections of u-net for medical image segmentation," *ArXiv*, vol. abs/2311.17791, 2023.

[14] A. Dosovitskiy, L. Beyer, A. Kolesnikov, D. Weissenborn, X. Zhai, T. Unterthiner, M. Dehghani, M. Minderer, G. Heigold, S. Gelly, J. Uszkoreit, and N. Houlsby, "An image is worth 16x16 words: Transformers for image recognition at scale," in *International Conference on Learning Representations*, 2021.

[15] A. Gu, K. Goel, and C. R'e, "Efficiently modeling long sequences with structured state spaces," *ArXiv*, vol. abs/2111.00396, 2021.

[16] A. Gu and T. Dao, "Mamba: Linear-time sequence modeling with selective state spaces," 2024.

[17] L. Zhu, B. Liao, Q. Zhang, X. Wang, W. Liu, and X. Wang, "Vision mamba: Efficient visual representation learning with bidirectional state space model," *ArXiv*, vol. abs/2401.09417, 2024.

[18] Y. Liu, Y. Tian, Y. Zhao, H. Yu, L. Xie, Y. Wang, Q. Ye, and Y. Liu, "Vmamba: Visual state space model," *ArXiv*, vol. abs/2401.10166, 2024.

[19] Z. Wang, J.-Q. Zheng, Y. Zhang, G. Cui, and L. Li, "Mamba-unet: Unet-like pure visual mamba for medical image segmentation," *ArXiv*, vol. abs/2402.05079, 2024.

[20] J. Ruan and S. Xiang, "Vm-unet: Vision mamba unet for medical image segmentation," *ArXiv*, vol. abs/2402.02491, 2024.

[21] J. Ruan and S. Xiang, "Vm-unet: Vision mamba unet for medical image segmentation," *ArXiv*, vol. abs/2402.02491, 2024.

[22] J. Ruan and S. Xiang, "Vm-unet: Vision mamba unet for medical image segmentation," *ArXiv*, vol. abs/2402.02491, 2024.

[23] J. Fu, J. Liu, H. Tian, Z. Fang, and H. Lu, "Dual attention network for scene segmentation," *2019 IEEE/CVF Conference on Computer Vision and Pattern Recognition (CVPR)*, pp. 3141–3149, 2018.

[24] Q. Hou, D. Zhou, and J. Feng, "Coordinate attention for efficient mobile network design," in *2021 IEEE/CVF Conference on Computer Vision and Pattern Recognition (CVPR)*, pp. 13708–13717, 2021.

[25] J. Park, S. Woo, J.-Y. Lee, and I.-S. Kweon, "Bam: Bottleneck attention module," *ArXiv*, vol. abs/1807.06514, 2018.

[26] D. Misra, T. Nalamada, A. U. Arasanipalai, and Q. Hou, "Rotate to attend: Convolutional triplet attention module," in *2021 IEEE Winter Conference on Applications of Computer Vision (WACV)*, pp. 3138–3147, 2021.

[27] F. Chollet, "Xception: Deep learning with depthwise separable convolutions," *2017 IEEE Conference on Computer Vision and Pattern Recognition (CVPR)*, pp. 1800–1807, 2016.

[28] N. C. F. Codella, D. Gutman, M. E. Celebi, B. Helba, M. A. Marchetti, S. W. Dusza, A. Kalloo, K. Liopyris, N. Mishra, H. Kittler, and A. Halpern, "Skin lesion analysis toward melanoma detection: A challenge at the 2017 international symposium on biomedical imaging (isbi), hosted by the international skin imaging collaboration (isic)," in *2018 IEEE 15th International Symposium on Biomedical Imaging (ISBI 2018)*, pp. 168–172, 2018.

[29] N. C. F. Codella, V. M. Rotemberg, P. Tschandl, M. E. Celebi, S. W. Dusza, D. Gutman, B. Helba, A. Kalloo, K. Liopyris, M. A. Marchetti, H. Kittler, and A. C. Halpern, "Skin lesion analysis toward melanoma detection 2018: A challenge hosted by the international skin imaging collaboration (isic)," *ArXiv*, vol. abs/1902.03368, 2019.

[30] I. Loshchilov and F. Hutter, "Decoupled weight decay regularization," in *International Conference on Learning Representations*, 2017.